Island Size Scaling in InAs/GaAs Self-Assembled Quantum Dots

Y. Ebiko, S. Muto, D. Suzuki, S. Itoh, K. Shiramine, and T. Haga
Department of Applied Physics, Hokkaido University, N13 W8 Kitaku, Sapporo 060 Japan

Y. Nakata and N. Yokoyama
Fujitsu Laboratories Ltd., 10-1 Morinosato-Wakamiya, Atsugi 243-01, Japan
(Received 22 July 1997)

We studied the cluster size distribution of dislocation-free InAs/GaAs self-assembled quantum dots obtained by the Stranski-Krastanow mode of molecular beam epitaxy. The same scaling function was obtained over a wide range of dot density. The scaling function indicated that the cluster size fluctuation, normalized by the average size, is constant for all the quantum dot densities studied. The resemblance of the scaling function to that of the submonolayer homoepitaxial growth implies that the strain is not the essential factor determining the cluster size distribution of quantum dots. [S0031-9007(98)05602-6]

PACS numbers: 68.55.–a, 61.43.Hv, 82.20.Mj

The growth of lattice-mismatch semiconductor systems such as Ge/Si and InAs/GaAs has been known to produce a dotlike structure by the Stranski-Krastanow (SK) mode. Recently this growth mode, especially of InAs/GaAs dots (known as "self-assembled quantum dots" [1]) has drawn much attention as a method to obtain quantum dots which are damage-free and fabrication-free. Now practical applications of quantum dots are seriously sought for, and efforts are being made in fabricating quantum dot lasers with predicted high performance such as a high characteristic temperature and a low threshold current. However, the current InAs quantum dots have a problem in size uniformity which is commonly about $\pm 10\%$, and is insufficient for laser applications. It is intriguing to know if this common size fluctuation is essential or accidental.

Not to mention practical applications, the scaling property of two-dimensional (2D) island size distribution is known for submonolayer coverage. According to the scaling assumption [2,3], the island distribution is given by

$$N_s = \frac{\theta}{\langle s \rangle^2} f(s/\langle s \rangle) . \tag{1}$$

Here N_s is the number of islands (normalized by the number of lattice sites) which contain s atoms, θ is the fractional surface coverage, $\langle s \rangle$ is the average number of atoms in an island, and $f(x)$ is the scaling function, which depends only on $s/\langle s \rangle$. This scaling assumption was confirmed experimentally in Fe homoepitaxy [4] and InAs/GaAs heteroepitaxy [5].

It is interesting to know if something similar to Eq. (1) holds for three-dimensional (3D) island growth by the SK mode, especially because it was reported [6] that the total island density ρ shows a power law as a function of the coverage expressed as

$$\rho = \rho_0(\theta - \theta_c)^{\alpha} \tag{2}$$

for θ from 1.5 to 1.9 monolayer (ML), where ρ_0 is the proportionality coefficient, θ_c is the critical coverage (1.5 ML), and the critical exponent α is 1.76. Equation (2) implies the presence of the scaling region and consequently the scaling function.

In this Letter, we present the 3D island size scaling which holds for a quite wide range of the total density of the dislocation-free InAs/GaAs islands by the SK mode.

The growth was done by the Riber 2300 molecular beam epitaxy (MBE) system on a nominally flat GaAs (001) substrate. After the growth of the GaAs buffer layer at a substrate temperature of 600 °C, growth was interrupted for 3–5 min, to decrease the temperature to 490 °C to obtain a $c(4 \times 4)$ surface, and the InAs was grown (at a rate of 0.1 μm/h with arsenic pressure of 5×10^{-6} Torr) without rotating the substrate. After the observation of a spotty pattern by reflection high energy electron diffraction (RHEED), the In shutter was closed and the sample was annealed for 60 s with the As shutter open, and the heating was stopped. The As shutter was kept open until the substrate was cooled down to about 300 °C. The islands were characterized by atmospheric atomic force microscopy (AFM) after the epiwafer was taken out of the MBE chamber. Three growth runs were used to obtain different coverage. To vary coverage, we also made use of the nonuniform growth rate of InAs while the substrate rotation was stopped. The coverage was deduced from the island density by using Eq. (2).

Figure 1 shows the AFM image of a low coverage sample where we could identify, in addition to 3D islands, large 2D islands (0.3 nm height), and quasi-3D islands (0.6–1.2 nm height) previously reported by using UHV STM/AFM [7]. Those 2D islands and quasi-3D islands were close to the resolution limit and not counted for the distribution. Figure 2 shows the average size (volume) of 3D islands, $\langle s \rangle$, as a function of the island density. The size initially increased to see a peak at about a density of 3×10^{10} cm^{-2} and then decreased as the island density increased. This kind of nonmonotonic density dependence

 0031-9007/98/80(12)/2650(4)$15.00

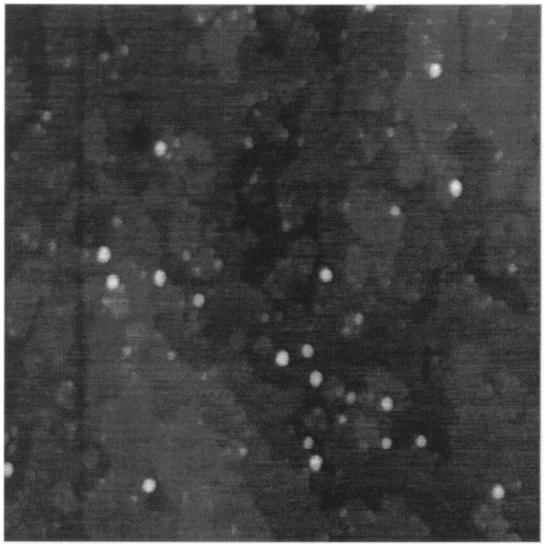

FIG. 1. A typical AFM image (1 μm $\times$ 1 μm) of low coverage ($\sim 2 \times 10^9$ cm^{-2}) sample. In addition to usual 3D islands (white spots), we can identify large 2D islands shown as gray platforms and quasi-3D islands (Ref. [7]) shown as small gray spots.

of size was also reported [8] but with a peak at much lower density. For samples with densities less than 3×10^{10} cm^{-2}, we could identify large 2D islands and quasi-3D islands as shown in Fig. 1. Therefore, these flat islands are regarded to be responsible for the reduction of the average size of 3D islands at ρ less than 3×10^{10} cm^{-2}.

Figure 3 shows the scaling function obtained for the 3D islands. Here the coverage θ was replaced by the value θ_{eff} deduced from the total island volume, that is, $\sum sN_s$. This subtracts the coverage used for the wetting layer. We did not specify the detailed shape of the 3D island. Instead we estimated the volume by the product of three values: lateral diameters of both [110] and [$\bar{1}$10] and the height. In fact, for a cone-shaped dot, the volume is $\frac{1}{3}$ of height $\times$ base area, and for a cap-shaped dot, the prefactor is $\frac{1}{2}$ considering the small aspect ratio (0.06–0.2; see Fig. 5 below). However, we note that the scaling function is independent of the prefactor of the volume unless different shapes such as cones and caps are mixed. The same scaling function was obtained over a wide range of island density. It is known that the dislocation formation [9] and the island coalescence [10] drastically widen the island-size distribution. Therefore, we believe that we are in a window of dislocation-free and coalescence-free growth condition in spite of the wide range of island density ρ we studied. It should be noted that there is no fitting parameter in these plots. Rather large deviations for samples with 2×10^{10} cm^{-2} (open square, and open circle) are regarded to be large fluctuations coming from a small (total) number of islands (about 100 for each).

The solid curve is the analytic expression [11] of 2D island distribution by submonolayer homoepitaxy with critical island size of 1. Again, there is no fitting parameter to obtain the curve. We note here that the analytic expression agreed quite well [11] with the computer simulation results as well as submonolayer homoepitaxy (Fe on Fe) experiments [4].

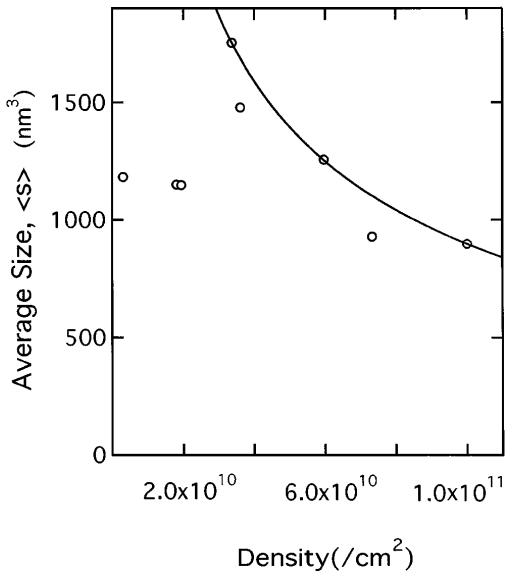

FIG. 2. Average cluster size $\langle s \rangle$ (height $\times$ $d(\bar{1}10) \times d(110)$ in units of nm^3), used to derive the scaling function. The solid curve is an eye guide. Below density of 3×10^{10} cm^{-2}, we could observe flat islands (large 2D islands and quasi-3D islands) shown in Fig. 1. These flat islands were not included in $\langle s \rangle$.

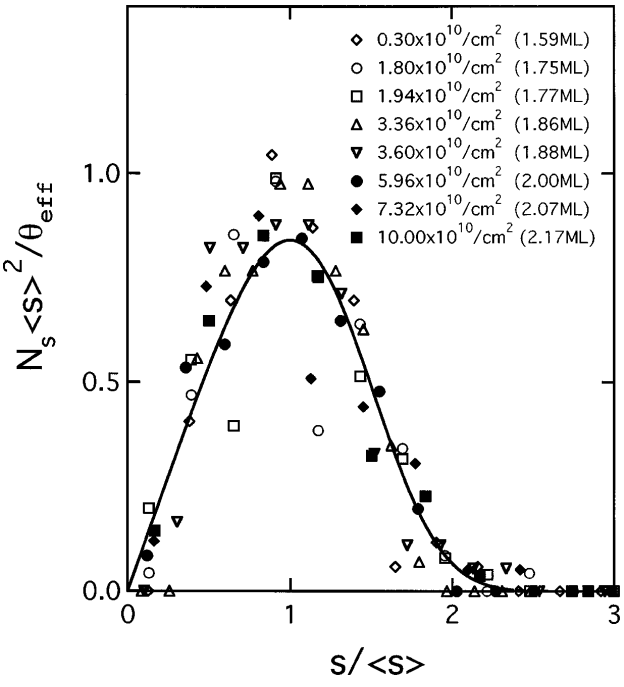

FIG. 3. The island size scaling function for a wide range of island density. The solid curve is the analytic expression given by Ref. [11].

Figure 4 shows the scaling function obtained from one lateral size, $d(\bar{1}10)$. Here, to compare with Fig. 3, the distribution of the lateral size was converted to volume (number of atoms, s) distribution by assuming that the island volume is proportional to $d(\bar{1}10)^3$. The scaling is much less clear. The difference between Figs. 3 and 4 suggests that the aspect ratio, height/lateral size, is not constant among 3D islands. In fact, Fig. 5 shows that the aspect ratio scatters from island to island even within the same sample. We believe that this is one of the reasons why the scaling function has not been reported for lateral size or height distribution of InAs/GaAs self-assembled quantum dots. We note here that the nonuniform aspect ratio is known for Ge/Si growth [12].

The scaling function of Fig. 3 indicates that size s of the 3D island is controlled by the surface dynamics of In atoms on InAs wetting layer, with a single scale of $\langle s \rangle$. This may appear surprising if we consider that the difference between the In in the wetting layer and In adatom is not clear especially because the wetting layer is not atomically flat. However, this kind of ambiguity is also present in a homoepitaxial growth experiment such as Fe on Fe substrate. More surprising is that, in the low density region of 2×10^{10} cm^{-2}, where large 2D islands and small quasi-3D islands [7] existed in addition to the 3D islands, the same scaling function was obtained. Moreover, the obtained scaling function was quite different from that of the 2D island of submonolayer heteroepitaxy of InAs on GaAs [5], but agreed to that of the 2D island of submonolayer homoepitaxy [4,11]. This is in favor of the mechanism proposed by Priester and Lannoo [13] on InAs/GaAs SK island which claims that the 2D islands on 1 ML wetting layer act as "precursors" for formation of 3D coherent island. However, our result in Fig. 3 excludes the presence of equilibrium or optimal distribution predicted by them. In addition, their mechanism predicts an increase in size as the coverage θ (or density ρ) is increased. This contradicts the decrease in size observed in Fig. 2. Instead, the agreement of the scaling function with that of submonolayer growth with critical island size of $i = 1$ suggests that In adatoms diffuse but dimers or larger clusters cannot move. If we adopt this simple picture, we can easily understand the decrease of the average size $\langle s \rangle$ observed in Fig. 2, as we increase the density ρ beyond 3×10^{10} cm^{-2}. As we increase coverage, the density ρ increases faster than proportional to $\theta - \theta_c$ as illustrated by Eq. (2). This is because the density is determined by the number of the nucleation sites which is formed by the nearest-neighbor collision of In adatoms. On the other hand, the product $\rho\langle s \rangle$ is the total volume of 3D islands and is $\theta - \theta_c$. Therefore, $\langle s \rangle$ should decrease as θ and ρ increase. For $\rho < 3 \times 10^{10}$ cm^{-2}, the above argument is not applicable because we have large 2D islands and quasi-3D islands which are not included in ρ and $\langle s \rangle$.

We note here two factors for ambiguity coming from atmospheric AFM measurements. First, the native oxide is present on the 3D island and wetting layer surfaces. This is believed to degrade the scaling function even if the thickness of the oxide is uniform. Second, due to the limited resolution, smaller 3D islands were not identified. We can see the trace of this cutoff in Fig. 3 at about 0.1

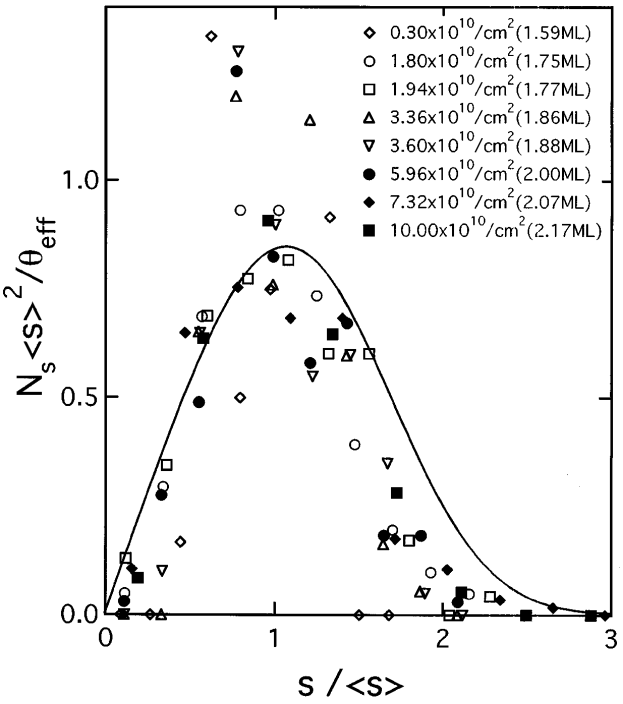

FIG. 4. The island size (volume) scaling function obtained from the lateral diameter $d(\bar{1}10)$ of 3D islands. Here, the size s was obtained by assuming $s \sim d(\bar{1}10)^3$.

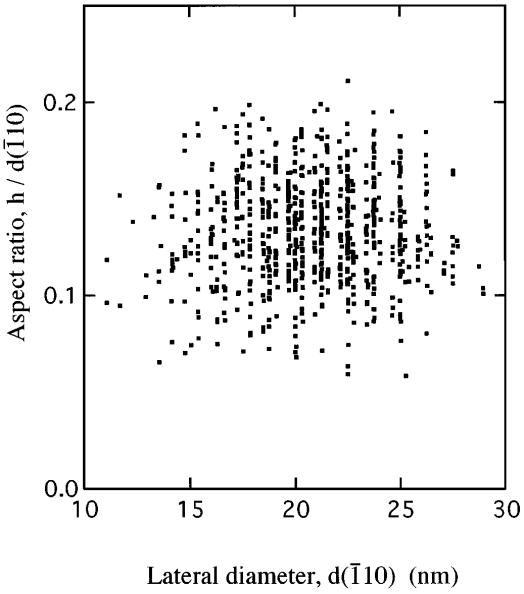

FIG. 5. The aspect ratio $h/d(\bar{1}10)$ as a function of $d(\bar{1}10)$, showing that the 3D islands are not proportional in size. Here, h denotes the height of 3D islands.

of the abscissa. This also works to degrade the scaling function by modifying the θ_{eff}. Besides, the measured lateral sizes are the upper bound of the actual dot size as is known [8] in scanning probe microscopy in general. The scaling function of Fig. 3 was obtained in spite of those nonideal circumstances.

Figure 3 tells us that the size fluctuation of 3D islands

$$\sqrt{(s - \langle s \rangle)^2}$$

decreased as $\langle s \rangle$ decreased when we increased the island density above 3×10^{10} cm^{-2}. This is consistent with previous reports [6,8,10,14] on the size distribution of 3D islands. However, Fig. 3 also tells us that the normalized fluctuation

$$\frac{\sqrt{(s - \langle s \rangle)^2}}{\langle s \rangle}$$

is constant all over the island density we studied, and that no specific mechanism is working to realize a uniform size distribution. This is puzzling if we consider the recent proposals of mechanism for homogeneously sized islands. One is the energy barrier [6,15,16] formed at the edge of a 3D island where the strain energy is maximum. Adatoms have to overcome this barrier to reach the island and thus the growth rate of 3D islands slows down as the size of the island becomes large. The other is the interaction of island induced strain field. Because of the interaction, when the island-island distance is not large, mass transport occurs from larger island to smaller island leading to uniform distribution of islands [8]. On the other hand, our scaling function is consistent with the homoepitaxial growth and its computer simulation which are free from strain effects, and the simulation even excluded the detachment process of adatoms. These imply that a strain-oriented mechanism was irrelevant to the 3D island distribution for ρ from 0.3 to 10×10^{10} cm^{-2} (estimated θ of 1.6 to 2.2 ML) under our growth conditions. It should be noted, however, that the strain did work to form 3D islands instead of 2D islands, but was not large enough to control the shape of the islands (see Fig. 5) and was irrelevant to their size distribution for the coverage we studied. This situation is somewhat similar to the simulation result [11] for submonolayer growth which showed that allowance of island edge diffusion of atoms (with only one bond to a 2D island) changed the island shape from fractal islands to compact islands without essential change in the scaling function.

Going back to the practical question, we can say that the size fluctuation we usually observe is essential and not accidental because it is natural to have the cluster size (or volume) distribution given in Fig. 3. However, if we look at lateral size, as we usually do, the distribution is not as reproducible, as seen in Fig. 4. We note that our lateral size distributions had width between $\pm(11-16)\%$, consistent with other reports.

In summary, we found a scaling function of cluster size of dislocation-free 3D island for InAs/GaAs self-assembled quantum dots obtained by the Stransky-Krastanow mode of MBE growth. The same scaling function was obtained over a wide range of 3D island density, and it indicated that the cluster size fluctuation normalized by the average size is constant for all the island density we studied. The resemblance of the scaling function to that of submonolayer homoepitaxial growth implies that the strain is irrelevant to the cluster size distribution of dislocation-free 3D islands.

The authors would like to express their sincere thanks to Professor H. Hasegawa and Dr. H. Fujikura, Research Center for Interface Quantum ELectronics (RCIQE), Hokkaido University, for allowing and instructing the use of the atomic force microscopy (Digital Instruments Inc. Nanoscope II) installed in the RCIQE facility. They are also grateful to Y. Horisaki and I. Toriumi for starting up our MBE system and to Professor Y. Abe for the encouragement of this line of work. This work was partially supported by a Grant-in-aid for Scientific Research from the Ministry of Education, Science, and Culture, Japan.

[1] D. Leonard, M. Krishnamurthy, C. M. Reaves, S. P. Denbaars, and P. M. Petroff, Appl. Phys. Lett. **63**, 3203 (1993).
[2] M. C. Bartelt and J. W. Evans, Phys. Rev. B **46**, 12 675 (1992).
[3] A.-L. Barabashi and H. E. Stanley, *Fractal Concepts in Surface Growth* (Cambridge University Press, Cambridge, England, 1995), p. 178.
[4] J. A. Stroscio and D. T. Pierce, Phys. Rev. B **49**, 8522 (1994).
[5] V. Bressler-Hill, S. Varma, A. Lorke, B. Z. Nosho, P. M. Petroff, and W. H. Weinberg, Phys. Rev. Lett. **74**, 3209 (1995).
[6] D. Leonard, K. Pond, and P. M. Petroff, Phys. Rev. B **50**, 11 687 (1994).
[7] T. R. Ramachandran, R. Heitz, P. Chen, and A. Madhukar, Appl. Phys. Lett. **70**, 640 (1997).
[8] N. P. Kobayashi, T. R. Ramachandran, P. Chen, and A. Madhukar, Appl. Phys. Lett. **68**, 3299 (1996).
[9] M. Krishnamurthy, J. S. Drucker, and J. A. Venables, J. Appl. Phys. **69**, 6461 (1991).
[10] J. M. Moison, F. Houzay, F. Barthe, L. Leprince, E. Andre, and O. Vatel, Appl. Phys. Lett. **64**, 196 (1994).
[11] J. G. Amar and F. Family, Phys. Rev. Lett. **74**, 2066 (1995).
[12] B. Voigtlaender and Andre Zinner, Appl. Phys. Lett. **63**, 3055 (1993).
[13] C. Priester and M. Lannoo, Phys. Rev. Lett. **75**, 93 (1995).
[14] A. Ponchert, A. LeCorre, H. L'Haridon, B. Lambert, and S. Salaun, Appl. Phys. Lett. **67**, 1850 (1995).
[15] Y. Chen and J. Washburn, Phys. Rev. Lett. **77**, 4046 (1996).
[16] A.-L. Barabashi, Appl. Phys. Lett. **70**, 2565 (1997).